

Research Article

STRUCTURAL ANALYSIS AND HOMOLGY MODELING OF MEMBERS OF SMT-LIKE OPERON FROM THERMOPHILIC CYANOBACTERIUM *THERMOSYNECHOCOCCUS ELONGATUS* BP-1

Rahul Mahadev Shelake^{1,2}, Hidenori Hayashi¹ and Eugene Hayato Morita^{2,3*}

¹Proteo-Science Center, Ehime University, Matsuyama, 7908577, Japan

²Molecular Cell Physiology Laboratory, Faculty of Agriculture, Ehime University, Matsuyama, 7908566, Japan

³Department of Chemistry, Faculty of Science, Josai University, Saitama, 3500295, Japan

Abstract: Whole genome sequencing of several cyanobacteria is recently completed and it offers a platform to explore metal homeostasis systems in further detail. In the present study, we mined genome of the hot spring cyanobacterium *Thermosynechococcus elongatus* BP-1 for metal sensors and metal-handling proteins. Detailed analysis of the genome data revealed a putative metal (zinc) homeostasis system (*tmt*) in *T. elongatus* BP-1 similar to that of *smt* operon in freshwater *Synechococcus* sp. PCC 7942. The *tmt* operon consists of two genes encoding a transcription regulator (TmtB) and metallothionein (TmtA). Also, transposase gene is exceptionally present in between TmtB and TmtA which is not observed in other *smt*-like operons. Amino acid sequence alignment confirmed that the TmtB shares higher similarity with SmtB (55%) from *Synechococcus* sp. PCC 7942 than another well-studied transcription regulator ZiaR (49%) from *Synechocystis* sp. PCC 6803. Also, important features of ArsR/SmtB family, such as metal-binding ligands and DNA-binding domain in TmtB are highly conserved. Alignment analysis of TmtA showed that the Cys-His residues involved in metal binding are highly conserved. Also, operator/promoter region of *tmtA* consists of an imperfect 12-2-12 inverted repeat which acts as a binding site for ArsR/SmtB transcription regulators. Furthermore, these findings are consistent with our experimental modeling data sets for the predicted secondary and tertiary structures for both the proteins.

Keywords: Cyanobacteria; SmtB/ArsR family; metal-responsive transcription factors; metallothioneins

Note: Coloured Figures available on Journal Website in "Archives" Section

Introduction

The oxygenic photosynthesis was first developed in cyanobacteria and molecular oxygen released in the process, had a large impact on our environment (Saito *et al.*, 2003; Raymond and Blankenship, 2004). Oxygen also played a major role in the evolutionary development of cyanobacteria and oceans which are closely connected and this also directed the distribution and utilization of metals. For metal ion speciation, fundamental as well as applied studies suggested

that the presence of oxygen increases the chances of decrease in availability of some metals such as iron, cobalt, nickel, and manganese. However, it also increases the bio-availability of zinc, copper, and cadmium (Blindauer, 2008). Such changes in metal ion chemistry led to physiological changes in cyanobacteria by evolution of metal-regulating proteins (Finney and O'Halloran, 2003). Therefore, cellular machinery of prokaryotes has evolved to act in response to changing metal ion concentrations in the surroundings and consists of two types of mechanisms. First one includes metallothioneins and another involves metal efflux proteins (Giedroc and Arunkumar, 2007). The expression of such metal-handling proteins is regulated by metal-responsive transcription

Corresponding Author: Eugene Hayato Morita

E-mail: ehmorita@josai.ac.jp

Received: September 13, 2016

Accepted: September 23, 2016

Published: September 26, 2016

factors. These transcription factors are the members of metalloregulatory ArsR/SmtB family and are present in oldest cyanobacteria such as *Gloeobacter* sp. (Nelissen *et al.*, 1995).

The members of ArsR/SmtB family consist of DNA-binding domains indispensable for metal ion homeostasis. These metal-responsive transcription factors regulate expression of either metallothioneins (intracellular sequestration), and/or metalloproteins (sequestration of metal ion or efflux across the periplasm) (Busenlehner *et al.*, 2003). Although many members of this family control the expression of either of the protein, Liu and co-workers (2004) demonstrated for the first time that a single transcription factor in *Oscillatoria brevis* regulates the expression of both a putative metal efflux pump and a metallothionein. In any of the case, they mediate the expression of metal-handling protein by binding to its operator/promoter region. Structural and functional studies of a metallothionein SmtA and its trans-acting repressor SmtB from *Synechococcus* sp. PCC 7942 provided thorough information about the functioning of metal-responsive mechanisms in cyanobacteria (Cook *et al.*, 1998; Busenlehner *et al.*, 2003; Shelake *et al.*, 2013a). Knowledge of metal ion sequestration, utilization and related mechanisms in hot spring species such as *Thermosynechococcus elongatus* BP-1 is very limited till date. Phylogenetic studies based on 16S rRNA sequences suggested *T. elongatus* BP-1 might be diverged at a very early time during evolution process of cyanobacteria (Honda *et al.*, 1999). *T. elongatus* BP-1 is being used as a model for studying various aspects of photosynthesis process (Henry *et al.*, 2016). It is a rod shaped unicellular photoautotrophic prokaryote with most favorable temperature for physiological growth 55°C. Whole genome of *T. elongatus* BP-1 is completely sequenced (Nakamura *et al.*, 2002) which is publicly available at CyanoBase and NCBI database.

In order to understand the metal-sensing mechanisms in thermophilic cyanobacterium, we mined whole genome sequence available at CyanoBase and found two SmtB homologues (locus tag: *tlr1018* and *tlr0769*). Previous studies about ArsR/SmtB members suggested that they

are often structured in operons along with metal-handling proteins, and they are transcribed divergently consisting common operator/promoter region (Busenlehner *et al.*, 2003; Blindauer, 2008; Shelake *et al.*, 2013a-b). Investigation of the neighboring genomic sequences of *tlr1018* locus revealed putative metal homeostasis system (termed *tmt* operon, Figure 1) similar to that of *smt* operon in *Synechococcus* sp. PCC 7942. This system appears to consist of a metallothionein denoted as TmtA (locus tag: *tsl1016*) and a SmtB homolog denoted as TmtB (locus tag: *tlr1018*). Exceptionally, a transposase coding gene (locus tag: *tlr1017*) was found in between TmtA and TmtB. Interestingly, transposase encoding gene and *tmtB* gene sequences shared 12 bp overlap.

The goal of present study was to explore structural and functional aspects of TmtA and TmtB using sequence alignment and homology-based protein models. Corresponding Cys-His residues in SmtA protein forming metal-binding domain are highly conserved in TmtA. Also, metal-binding sites and DNA-binding motif of TmtB are highly conserved and identical to that of SmtB. The secondary (2D) and tertiary (3D) structures of both the proteins were built using online platform- Protein Homology/analog Y Recognition Engine version 2 (Phyre2), one of the most referred tool for structure prediction (Kelley *et al.*, 2015). Both the models were deposited in protein model database without any changes (Castrignano *et al.*, 2006). These models can be accessed at PMDB identifiers PM0080611 for TmtA and PM0080610 for TmtB. In general, predicted 3D models for TmtA and TmtB are compatible with the findings of sequence alignment analysis and are discussed in detail.

Material and Methods

Identification of SmtB homologs and chromosomal localization

Sequences of the putative ArsR/SmtB members were identified employing BLAST searches for SmtB from genome of *T. elongatus* BP-1 available at CyanoBase website (http://genome.microbedb.jp/blast/blast_search/cyanobase/Thermo/genes) of Kazusa genome

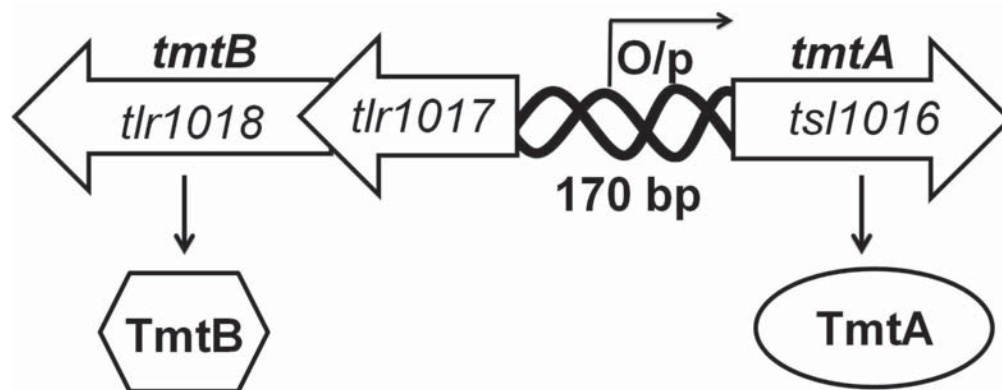


Figure 1: Schematic representation of *tmt* operon from *T. elongatus* BP-1. The transposase gene is present in between transcriptional repressor gene (*tmtB*) and metallothionein gene (*tmtA*). The locus tags of respective genes are mentioned inside the arrows.

resources. The localization of annotated SmtB homologs was determined on a bacterial chromosome and their neighboring sequences were screened for genes encoding metal-handling proteins.

Sequence alignment analysis

TmtA and TmtB proteins were aligned with the online tool Toffee@igs (<http://igs-server.cnrs-mrs.fr/Tcoffee/>) automatically (Notredame *et al.*, 2000; Poirot *et al.*, 2003) for checking the conserved sequences. Multiple sequence alignment was done using ClustalX 1.83 program (Altschul *et al.*, 1997) with default parameters and the initial alignments were refined manually by visual inspection.

Secondary and tertiary structure prediction

Protein structure predictions were performed using online tool Phyre2 (pronounced as 'fire') available on the webpage: <http://www.sbg.bio.ic.ac.uk/~phyre2> (Kelley *et al.*, 2015). Phyre2 could predict the secondary as well as tertiary structure adopted by a user-supplied protein sequence without additional configuration. Total 131 amino acid sequence of TmtB and the whole sequence of TmtA (57 amino acids) was applied to Phyre2 server separately. After alignment several templates (mostly from superfamily: "Winged helix" DNA-binding domain) were selected by Phyre2 to model the 3D structures of TmtB. The 3D structure of TmtA was modeled by Phyre2 and aligned templates

were selected from metallothionein super-family. Additionally, 3D structures of TmtA and TmtB were predicted using SWISS-MODEL modeling server (<http://swissmodel.expasy.org/>) accessible via either DeepView program or ExPASy web server (Arnold *et al.*, 2006). Online tool named 3DLigand-Site (<http://www.sbg.bio.ic.ac.uk/~3dligandsite/>) was used to predict the zinc binding sites in predicted TmtB model (Wass *et al.*, 2010). Recent version (v.1.8) of UCSF Chimera (<http://www.cgl.ucsf.edu/chimera/>) was used for interactive visualization and 3D structure analysis of predicted models (Pettersen *et al.*, 2004).

Results and Discussion

Comparative analysis of operator/promoter region of *tmtA*

The structures of all studied operons responsive to metal ions consist of one or two imperfect 12-2-12 inverted repeats (Busenlehner *et al.*, 2003). These repeats are normally positioned near or overlapping the starting point of transcription of the gene encoding metal-handling protein. The *smt* operon has two 12-2-12 inverted repeats termed 'Bbs1' and 'Bbs2' (Morita *et al.*, 2002). In case of operator/promoter of *tmtA* gene, only one inverted repeat (GACGTATGAACA-GT-TGTTCAAGTATA) was present just at the beginning of TATA box showing significant nucleotide sequence identity with Bbs2 from SmtB/SmtA (Figure 2). This nucleotide sequence of 12-2-12 inverted repeat was compared with

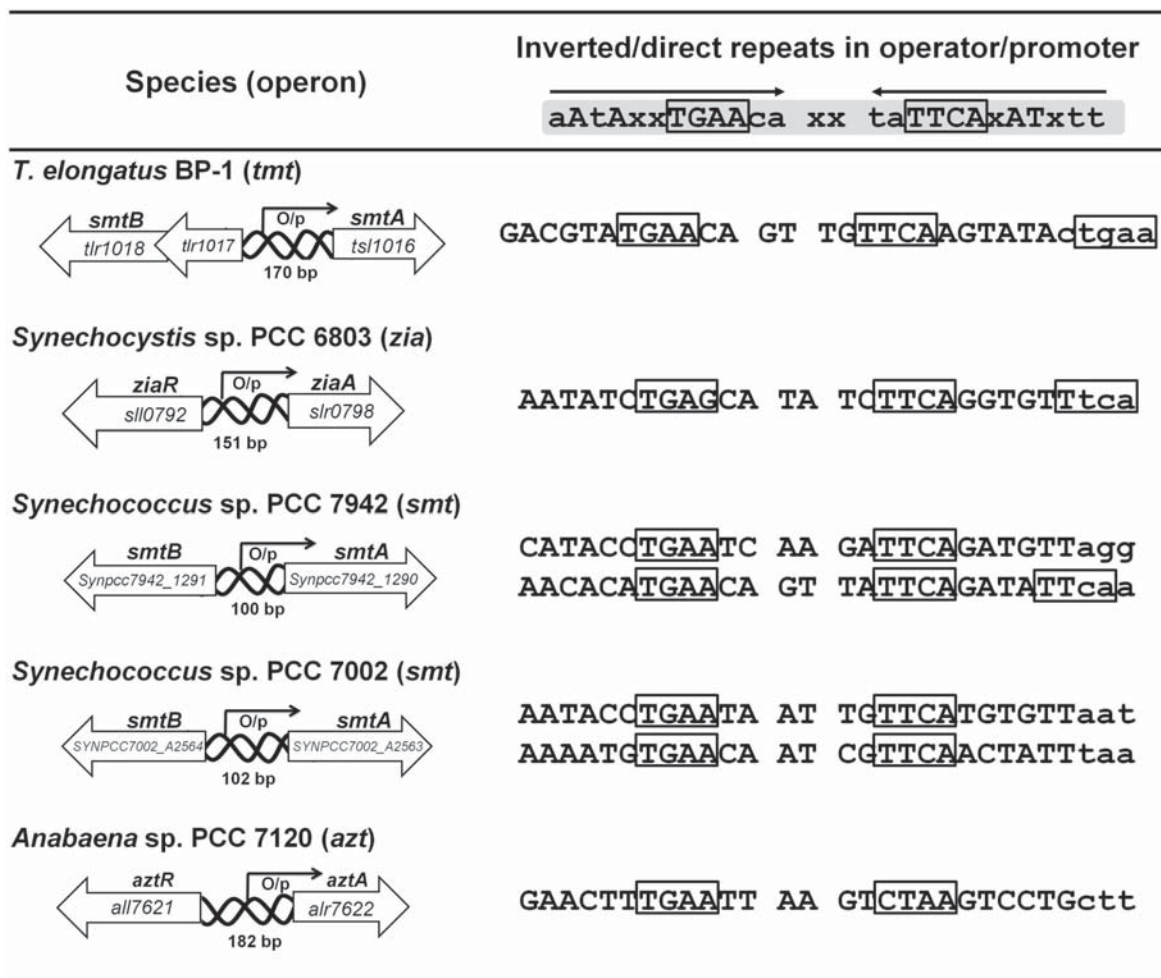


Figure 2: Comparison between 12-2-12 inverted repeats of operator/promoter regions in *smt*-like operons from different cyanobacterial species. Locus tags in cyanobase database for respective genes are mentioned inside the arrows. Highly conserved bases (TGAA and TTCA) are highlighted in box.

operator/promoter regions of similar operons present in several cyanobacterial species. The extra direct repeat TTCA is previously reported in ZiaR/ZiaA (*Synechocystis* sp. PCC 6803) and SmtB/SmtA (*Synechococcus* sp. PCC 7942). This variation in operator/promoter region have an effect on binding affinity of transcription repressor resulting differential tolerance levels to zinc ion stress (Shelake *et al.*, 2013a). Extra direct repeat (TGAA) present only in TmtB/TmtA may have a crucial role in differential responses to metal ion sensitivity in *T. elongatus*. To certify above findings about TmtB (transcriptional regulator) and TmtA (metallothionein), 2D and 3D structures were built for TmtA and TmtB using online software Phyre2 and SWISS-MODEL. For both proteins, predicted structures with Phyre2 and SWISS-MODEL were significantly same,

therefore only Phyre2 results are discussed in detail.

Sequence alignment analysis of TmtA

Tcoffee analysis with Toffee@igs confirmed high score (99) for TmtA with SmtA indicating highly conserved structural similarities. The amino acid sequence similarity of TmtA with SmtA was found to be 53%. The solution NMR structure of SmtA from *Synechococcus* sp. PCC 7942 has revealed that SmtA monomer can bind up to four zinc ions abbreviated as Zn₄SmtA (Blindauer *et al.*, 2007). Sequence alignment of TmtA with SmtA (Figure 3A) clearly demonstrated that all corresponding Cys and His residues in TmtA are identical with the single exception of His40 compared to that of SmtA. His40 in TmtA is replaced by Cys and displaced to 41th position.

As shown in Figure 3C, structure of Zn_4 SmtA involves nine Cys thiolate sulfurs (Cys9, Cys11, Cys14, Cys16, Cys32, Cys36, Cys47, Cys52, and Cys54) and two His imidazole nitrogens (His40 and His49). The site shown in red is the most accessible site for metal-binding in SmtA, and it is also the most variable site in the metallothionein family (Blindauer *et al.*, 2001). The coordinating His residues in structure of zinc bound SmtA are responsible for a balanced charge of zinc cluster in metalated protein and provide stable metal bound reactivity. This also protect zinc cluster from oxidizing agents (Blindauer *et al.*, 2007). This co-ordination geometry of His residues also provides a higher specificity for zinc than any other divalent metal ions. Presence of extra His13 and absence of His55 in TmtA sequence may have a crucial role in stabilizing the core zinc finger cluster.

Analysis of 2D and 3D models of *TmtA*

For TmtA, predicted secondary structure shown significant amounts of disorder (60%) in amino acid sequence (Figure 3B). Even though a higher percentage of disorder was present in amino acid sequence, 88% of residues of TmtA were modeled at >99% confidence for predicted 3D structure. In order to determine the 3D structure of TmtA protein, two templates sharing 54% sequence identity, named d1jjda (metallothionein fold) and c1jjda (PDB ID-1JJJ, NMR structure of the cyanobacterial metallothionein SmtA from *Synechococcus* sp. PCC 7942) were chosen automatically based on percentage identity, alignment coverage and heuristics to maximize confidence. With these two templates, 50 residues (5-54) were modeled from TmtA with more than 99.9% confidence and 7 residues were modeled by *ab initio* method. The *ab initio* is a *De novo* method that need enormous computational resources, and thus generally possible only for comparatively small proteins like TmtA.

The 3D model of TmtA is shown in Figure 3D. All Cys-His residues are labeled and relative positions of zinc ions in comparison to SmtA (PDB ID- 1JJJ) are drawn in the model. Even though side chains of all Cys-His involved in tetrahedral metal ion geometry are not in the same orientation as of SmtA, relative positions of Cys-

His residues forming the characteristic zinc finger fold were same. Previous studies have reported very little amount of amino-acid sequence identity among all studied metallothioneins in prokaryotes as well as in other kingdoms (Blindauer *et al.*, 2010). Divergent sequences of metallothioneins in different organisms make it more complex to understand their evolutionary development (Barnett *et al.*, 2012). Conservation of Cys-His residues forming zinc finger fold in TmtA might have reflected in 3D structure prediction in Phyre2 tool. Consequently, orientation of Cys-His residues in TmtA may generate higher or less number of metal-binding sites with difference in metal-binding affinities at each site (Barnett *et al.*, 2012).

Sequence alignment analysis of *TmtB*

Amino acid sequence of TmtB was more closely related with SmtB with sequence identity of 55% than ZiaR with sequence identity of 49% (Figure 4A). Multiple sequence alignment of TmtB with SmtB and ZiaR was performed in ClustalX program (Altschul *et al.*, 1997). Even though TmtB protein shows higher similarity with SmtB and ZiaR, there was a major difference in the N-terminal region. Previous studies have shown that at least two distinct metal-binding sites are present in SmtB homodimer from *Synechococcus* sp. PCC 7942 (VanZile *et al.*, 2002a; Busenlehner *et al.*, 2002; VanZile *et al.*, 2002b; Morita *et al.*, 2002). These metal-binding sites were denoted as the $\alpha 3$ (or $\alpha 3N$) and $\alpha 5$ sites (Figure 4B). The corresponding residues that are expected to be the ligands for Zn^{2+} are mostly but not completely conserved in putative $\alpha 5$ and $\alpha 3N$ sites of TmtB (Figure 4B). In addition, helix-turn-helix (HTH) motif is also highly conserved (15 out of 21 amino acids, 71%) and amino acid residues forming HTH motif are highlighted in gray shade along with dotted line at upper side (Figure 4A). This HTH region of TmtB protein might involved in direct interaction with operator/promoter region of TmtA as previously reported for SmtB (Busenlehner *et al.*, 2003).

The 2D and 3D structure prediction-analysis of *TmtB*

The 2D structure predicted using Phyre2 for the TmtB confirmed five alpha (α) helices and two

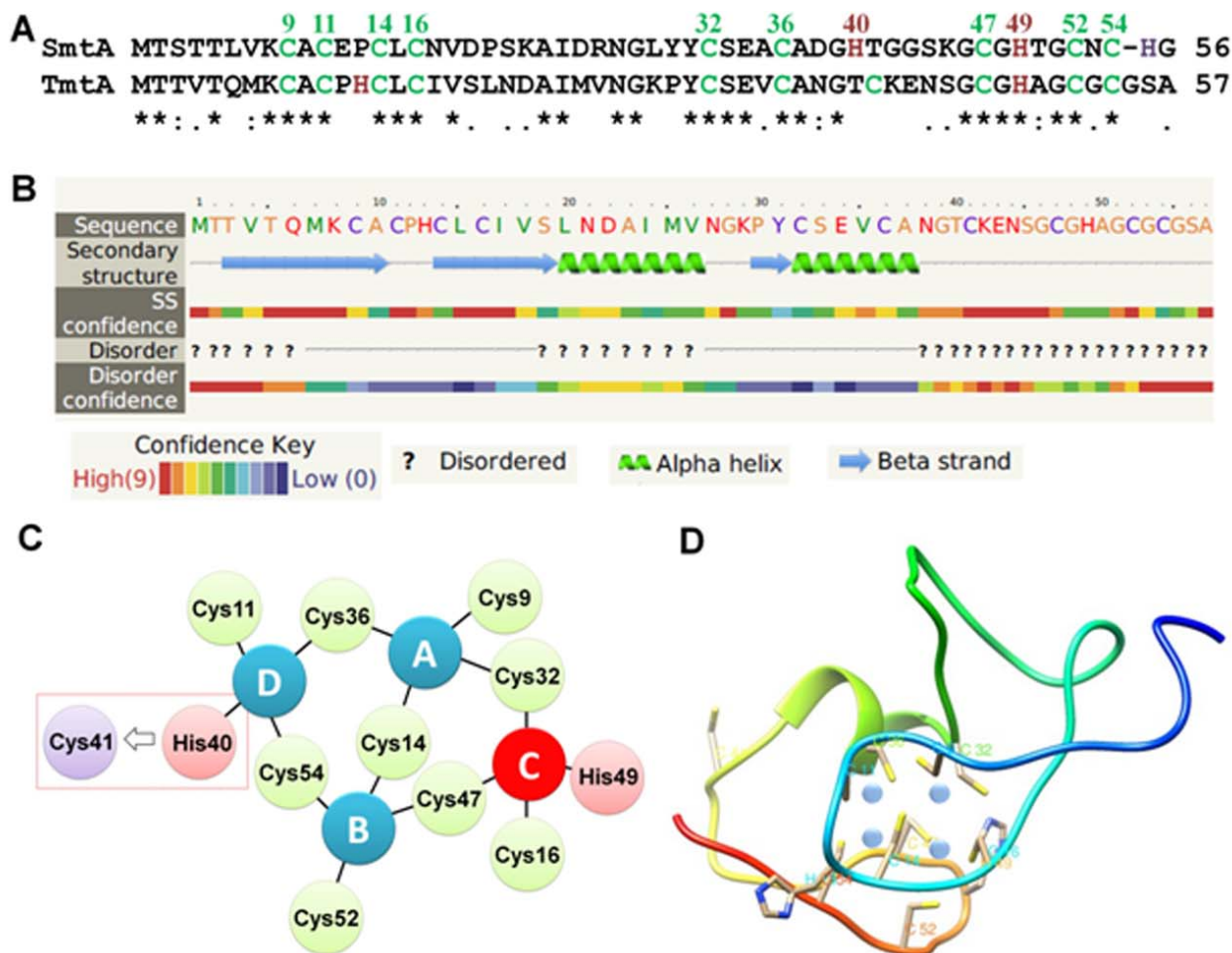


Figure 3: Sequence alignment, 2D and 3D models of TmtA. **A.** Pairwise alignment of TmtA with SmtA performed in ClustalX program. Cys and His residues are highlighted in green and red respectively. Conserved amino acids are depicted with asterisks (*); amino acids having same properties are shown with semicolon (;), and partly degenerated are indicated with a period (.). **B.** Each amino acid in 2D model is colored based on fundamental properties- yellow: small/polar (G,P,T,A,S); green: hydrophobic (V,M,I,L); red: charged (N,D,H,Q,K,R,E) and purple: Cys + aromatic (F,C,W,Y). Predicted disordered areas indicated by question marks. 'SS' (secondary structure) confidence level is indicated with rainbow color-code: red depict highest confidence and blue depict lowest confidence. **C.** Representation of metal-binding ligands forming zinc ion cluster in TmtA. Zinc ions are drawn in blue or red circles. Cys residues are drawn in light green and His residues in pink. The displacement of His40 in TmtA with Cys41 was highlighted in red dotted box. **D.** TmtA model generated by Phyre2. Relative positions of zinc ions are shown with blue circles.

beta (β) strands, consisting folds of $\alpha 1$ - $\alpha 2$ - $\alpha 3$ - $\alpha 4$ - $\beta 1$ - $\beta 2$ - $\alpha 5$ which is quite same to that of SmtB from *Synechococcus* sp. PCC 7942. The 3D structure prediction for TmtB using Phyre2 was performed at intensive modeling mode. Total 96 amino acid residues (from 31 to 126: 73% of TmtB sequence) were modeled with 99.94% confidence. Total 20 models were proposed by comparative modeling with already known 3D structures of related proteins with <99.94% confidence. The ultimate proposed model was monomer (Figure 5A) and generated automatically on the basis of two templates having <52% sequence identity. First

template c1r22B denoting a transcription repressor SmtB [PDB ID and Title: 1R22, SmtB (C14S/C61S/C121S mutant) in the $Zn_2\alpha_5$ -form]; and other d1r1ta denotes ArsR-like transcriptional regulators (PDB ID and Title: 1R1T, SmtB in the apo-form).

Secondary structural view (pipe and planks) of modeled TmtB generated in FirstGlance Jmol online tool (<http://bioinformatics.org/firstglance/fgij/>) showed similar pattern as predicted in Phyre2 program (Figure 5B). In order to know the structural similarity with original templates selected for modeling, comparative

analysis in chimera program was performed for modeled TmtB and original PDB models (1R22, 1R1T) independently. The obtained results of superimposed images are summarized in Figure 5C and 5D. In case of both the superimposed models, 'winged helix' DNA-binding domain in modeled TmtB showed high similarities with PDB structures. The major difference was observed in the N-terminal region which was predicted using *ab initio* method. The first 29 amino acids in both original PDB structures (1R22, 1R1T) were not observed in electron density maps, and this region was manually added to finally derived structures (Cook *et al.*, 1998). Therefore, position of N-terminal region in modeled TmtB may have some other possible confirmations and hence prediction of $\alpha 3N$ site for Zn^{2+} binding may not be reliable.

We further analyzed $\alpha 5$ site in modeled TmtB (Figure 8E-G) with 3DLigand-Site (online tool).

Two amino acid residues in $\alpha 5$ site of SmtB are derived from the $\alpha 5$ helix of one subunit (Asp104 and His106) and two other derived from the $\alpha 5$ helix of the other (His117 and Glu120) (Eicken *et al.*, 2003). On the basis of superimposed model studies and sequence alignment, we propose the corresponding residues forming $\alpha 5$ site in TmtB are Asp109, His111 from one monomer and His122, Glu125 from the other one (Figure 8E). Relative positions of side chains from Asp109 and His111 in TmtB were in same orientation as that of Asp104 and His106 in SmtB (Figure 8F and 8G) and similar was the case for His122 and Glu125.

The theoretical methods of structure prediction and homology modeling of proteins are depend on the general idea that 3D structure of a protein and its confirmation is highly preserved than its sequence of amino acids and small or intermediate alteration in amino acids may cause small or no change in the higher order

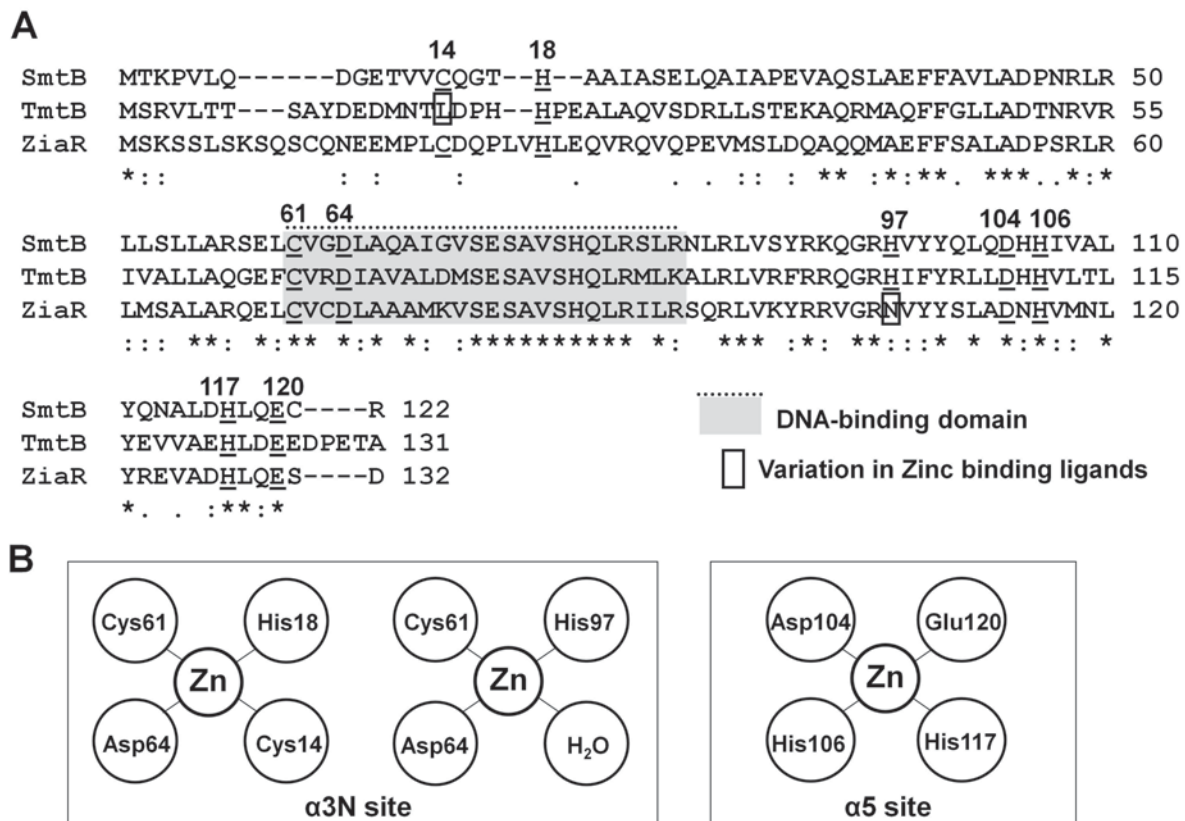


Figure 4: A. Multiple sequence alignment of TmtB with SmtB and ZiaR done using ClustalX program. Putative metal-binding legands corresponding to $\alpha 3N$ and $\alpha 5$ sites are underlined. The dissimilar amino acids as metal-binding ligands in TmtB as compared to SmtB are highlighted in box. B. Amino acid residues forming metal-binding sites in SmtB from *Synechococcus* sp. PCC 7942.

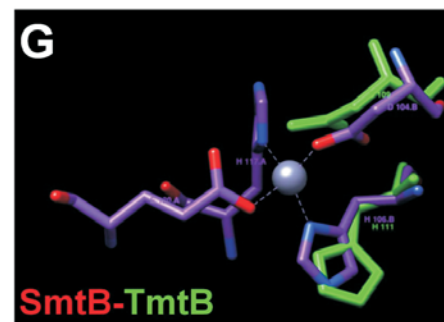
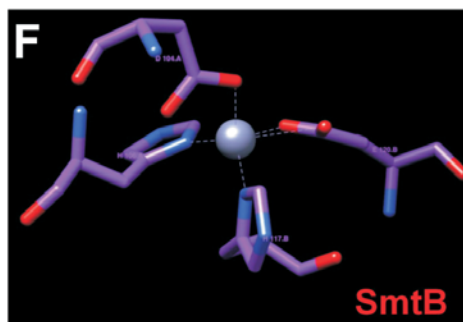
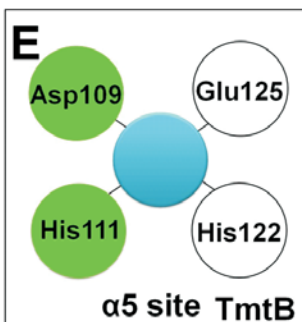
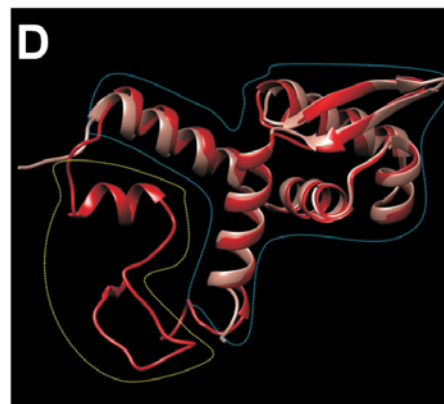
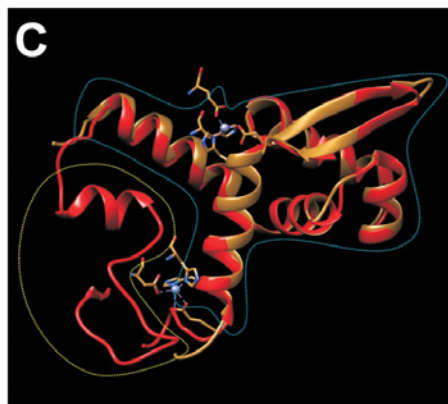
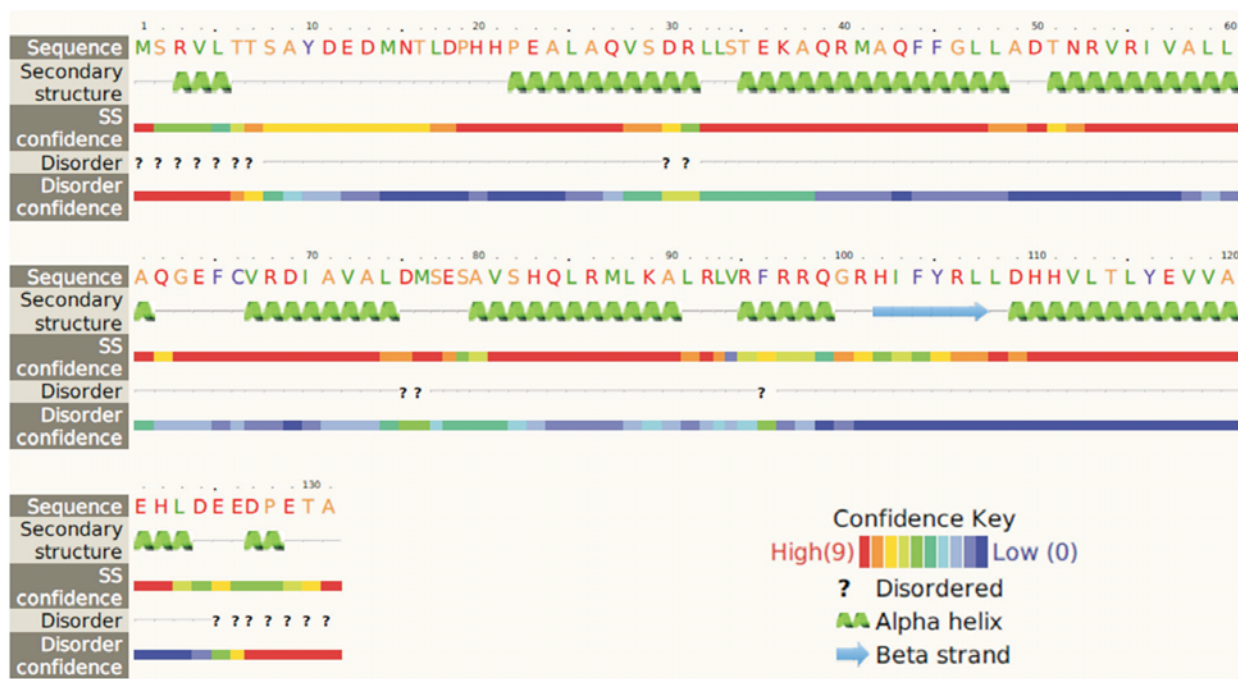
A

Figure 5: A. Secondary structure predicted for TmtB. Color schemes for amino acids and confidence level for each prediction is same as mentioned for TmtA model. B. Features of 2D structure ($\alpha 1$ - $\alpha 2$ - $\alpha 3$ - $\alpha 4$ - $\beta 1$ - $\beta 2$ - $\alpha 5$ folds) are shown in modeled TmtB. C. The superimposed image of TmtB model with zinc-bound SmtB mutant (PDB ID: 1R22). Highly variable N-terminal region is shown in yellow dotted box and conserved winged helix motif and other portion is highlighted in blue dotted box. D. The superimposed image of TmtB model with Apo-SmtB (PDB ID: 1R1T). E. Graphic model of $\alpha 5$ site in TmtB. The $\alpha 5$ site include Asp109, His111 residues from one monomer; His122, Glu125 from the other one. F. Orientation of zinc ion and side chains of amino acid residues in $\alpha 5$ site of SmtB dimer. G. The superimposed image of side chains of amino acids forming $\alpha 5$ site from modeled TmtB monomer (Asp109 and His111) with $\alpha 5$ site of SmtB dimer is shown.

structure of protein. In general, building of trustworthy homology models are possible if the similarity of template and query sequences is more than 30% (Marti-Renom *et al.*, 2000). Further experimental analysis with crystallographic and/or NMR studies of *tmt* operon containing *TmtA* (metallothionein) and *TmtB* (ArsR/SmtB family member) will definitely help to understand the structural and functional aspects.

Conclusions

Analysis of *tmt* locus from the hot spring cyanobacterium *Thermosynechococcus elongatus* BP-1 performed using bioinformatic tools that revealed *tmt* operon encoding a metal homeostasis system. Previously reported 'signature sequence' (imperfect 12-2-12 inverted repeat) in all metal-responsive operons is present in the operator/promoter region of *tmtA* suggesting similar mechanism of gene regulation. Cys-His residues associated with zinc finger fold in *SmtA* are highly conserved in protein *TmtA* and modeled 3D structure also strongly supports the *TmtA* function as a metallothionein. The sequence analysis and modeled 3D structure of *TmtB* protein verified distinctive features of ArsR/SmtB family members such as highly conserved distinct metal-binding sites and DNA binding domain (HTH motif). This intensive bioinformatic analysis of *tmt* operon in *T. elongatus* BP-1 will help to instigate investigation of metal ion sensing in extreme environment.

Acknowledgments

Authors are grateful to MEXT (Ministry of Education, Culture, Sports, Science and Technology in Japan) for providing doctoral fellowship to R.M.S.

Abbreviations

BLAST, Basic Local Alignment Search Tool; PDB, Protein Data Bank; Phyre, Protein Homology/analog Y Recognition Engine; 2D, Two dimensional; 3D, Three dimensional.

Conflict of interest

The authors declare that there is no conflict of interest with the contents of this article.

References

Altschul, S.F., Madden, T.L., Schäffer, A.A., Zhang, J., Zhang, Z., Miller, W. and Lipman, D.J. (1997). Gapped BLAST and PSI-BLAST: a new generation of protein

- database search programs. *Nucleic Acids Res.* 25, 3389–3402.
- Arnold, K., Bordoli, L., Kopp, J. and Schwede, T. (2006). The SWISS-MODEL Workspace: A web-based environment for protein structure homology modeling. *Bioinformatics* 22, 195–201.
- Barnett, J.P., Millard, A., Ksibe, A.Z., Scanlan, D.J., Schmid, R. and Blindauer, C.A. (2012). Mining genomes of marine cyanobacteria for elements of zinc homeostasis. *Front Microbiol.* 3, 142.
- Blindauer, C.A. (2008). Zinc-handling in cyanobacteria: an update. *Chem. Biodivers.* 5, 1990–2013.
- Blindauer, C.A., Harrison, M.D., Parkinson, J.A., Robinson, A.K., Cavet, J.S., Robinson, N.J. and Sadler, P.J. (2001). A metallothionein containing a zinc finger within a four-metal cluster protects a bacterium from zinc toxicity. *Proc. Natl. Acad. Sci. U.S.A.* 98, 9593–9598.
- Blindauer, C.A. and Leszczyszyn, O.I. (2010). Metallothioneins: unparalleled diversity in structures and functions for metal ion homeostasis and more. *Nat. Prod. Rep.* 27, 720–741.
- Blindauer, C.A., Razi, M.T., Campopiano, D.J. and Sadler, P.J. (2007). Histidine ligands in bacterial metallothionein enhance cluster stability. *J. Biol. Inorg. Chem.* 12, 393–405.
- Busenlehner, L.S., Pennella, M.A. and Giedroc, D.P. (2003). The SmtB/ArsR family of metalloregulatory transcriptional repressors: Structural insights into prokaryotic metal resistance. *FEMS Microbiol. Rev.* 27, 131–143.
- Busenlehner, L.S., Weng, T.C., Penner-Hahn, J.E. and Giedroc, D.P. (2002). Elucidation of primary (α 3N) and vestigial (α 5) heavy metal binding sites in *Staphylococcus aureus* pI258 CadC: evolutionary implications for metal ion selectivity of ArsR/SmtB metal sensor proteins. *J. Mol. Biol.* 319, 685–701.
- Castrignano T., De Meo P.D., Cozzetto D., Talamo I.G., Tramontano A. (2006). The PMDB Protein Model Database. *Nucleic Acids Res.* 34, 306–309.
- Cook, W.J., Kar, S.R., Taylor, K.B. and Hall, L.M. (1998). Crystal structure of the cyanobacterial metallothionein repressor SmtB: A model for metalloregulatory proteins. *J. Mol. Biol.* 275, 337–346.
- Eicken, C., Pennella, M.A., Chen, X., Koshlap, K.M., VanZile, M.L., Sacchettini, J.C. and Giedroc, D.P. (2003). A metal-ligand-mediated intersubunit allosteric switch in related SmtB/ArsR zinc sensor proteins. *J. Mol. Biol.* 333, 683–695.
- Finney, L.A. and O'Halloran, T.V. (2003). Transition metal speciation in the cell: insights from the chemistry of metal ion receptors. *Science* 300, 931–936.
- Giedroc, D.P. and Arunkumar, A.I. (2007). Metal sensor proteins: nature's metalloregulated allosteric switches. *Dalton Trans.* 29, 3107–3120.
- Henry, C.S., Bernstein, H.C., Weisenhorn, P., Taylor, R.C., Lee, J.Y., Zucker, J. and Song, H.S. (2016). Microbial Community Metabolic Modeling: A Community Data

- Driven Network Reconstruction. *J Cell Physiol.* 231, 2339–2345.
- Honda, D., Yokota, A. and Sugiyama, J. (1999). Detection of seven major evolutionary lineages in cyanobacteria based on the 16S rRNA gene sequence analysis with new sequences of five marine *Synechococcus* strains. *J. Mol. Evol.* 48, 723–739.
- Kelley, L.A., Mezulis, S., Yates, C.M., Wass, M.N. and Sternberg, M.J. (2015). The Phyre2 web portal for protein modeling, prediction and analysis. *Nat. Protoc.* 10, 845–858.
- Liu, T., Nakashima, S., Hirose, K., Shibasaka, M., Katsuhara, M., Ezaki, B., Giedroc, D.P. and Kasamo, K. (2004). A novel cyanobacterial SmtB/ArsR family repressor regulates the expression of a CPx-ATPase and a metallothionein in response to both Cu(I)/Ag(I) and Zn(II)/Cd(II). *J. Biol. Chem.* 279, 17810–17818.
- Marti-Renom, M.A., Stuart, A.C., Fiser, A., Sanchez R., Melo, F. and Sali, A. (2000). Comparative protein structure modeling of genes and genomes. *Annu. Rev. Biophys. Biomol. Struct.* 29, 291–325.
- Meyer, B. and Kuever, J. (2008). Homology modeling of dissimilatory APS reductases (AprBA) of sulfur-oxidizing and sulfate-reducing prokaryotes. *PLoS One* 3, e1514.
- Morita, E.H., Wakamatsu, M., Uegaki, K., Yumoto, N., Kyogoku, Y. and Hayashi, H. (2002). Zinc ions inhibit the protein-DNA complex formation between cyanobacterial transcription factor SmtB and its recognition DNA sequences. *Plant Cell Physiol.* 43, 1254–1258.
- Nakamura, Y., Kaneko, T., Sato, S., Ikeuchi, M., Katoh, H., Sasamoto, S., Watanabe, A., Iriguchi, M., Kawashima, K., Kimura, T., Kishida, Y., Kiyokawa, C., Kohara, M., Matsumoto, M., Matsuno, A., Nakazaki, N., Shimpo, S., Sugimoto, M., Takeuchi, C., Yamada, M. and Tabata, S. (2002). Complete genome structure of the thermophilic cyanobacterium *Thermosynechococcus elongatus* BP-1. *DNA Res.* 9, 123–130.
- Nelissen, B., Van de Peer, Y., Wilmotte, A. and De Wachter, R. (1995). An early origin of plastids within the cyanobacterial divergence is suggested by evolutionary trees based on complete 16S rRNA sequences. *Mol. Biol. Evol.* 12, 1166–1173.
- Notredame, C., Higgins, D.G. and Heringa, J. (2000). T-Coffee: A novel method for fast and accurate multiple sequence alignment. *J. Mol. Biol.* 302, 205–217.
- Pettersen, E.F., Goddard, T.D., Huang, C.C., Couch, G.S., Greenblatt, D.M., Meng E.C. and Ferrin, T.E. (2004). UCSF Chimera—a visualization system for exploratory research and analysis. *J. Comput. Chem.* 25, 1605–1612.
- Poirot, O., O'Toole, E. and Notredame, C. (2003). Tcoffee@igs: A web server for computing, evaluating and combining multiple sequence alignments. *Nucleic Acids Res.* 31, 3503–3506.
- Raymond, J. and Blankenship, R.E. (2004). The evolutionary development of the protein complement of photosystem 2. *Biochim. Biophys. Acta* 1655, 133–139.
- Saito, M.A., Sigman, D.M. and Morel, F.M.M. (2003). The bioinorganic chemistry of the ancient ocean: the co-evolution of cyanobacterial metal requirements and biogeochemical cycles at the Archean-Proterozoic boundary? *Inorg. Chim. Acta* 356, 308–318.
- Shelake, R.M., Aibara, K., Hayashi, H., Abe, S. and Morita, E.H. (2013). Comparative analysis of heavy-metal ion sensing mechanisms with transcription factors, smtbs, from freshwater *Synechococcus* sp. PCC 7942 and marine *Synechococcus* sp. PCC 7002: evolutionary and structural aspects. *IJSTR* 2, 274–284.
- Shelake, R.M., Hayashi, H., Ikegami, I., Abe, S. and Morita, E.H. (2013). Improved protein overexpression and purification strategies for structural studies of cyanobacterial metal-responsive transcription factor, SmtB from marine *Synechococcus* sp. PCC 7002. *The Protein J.* 32, 626–634.
- VanZile, M.L., Chen, X. and Giedroc, D.P. (2002). Allosteric negative regulation of smt O/P binding of the zinc sensor, SmtB, by metal ions: a coupled equilibrium analysis. *Biochemistry* 41, 9776–9786.
- VanZile, M.L., Chen, X. and Giedroc, D.P. (2002). Structural characterization of distinct α 3N and α 5 metal sites in the cyanobacterial zinc sensor SmtB. *Biochemistry* 41, 9765–9775.
- Wass, M.N., Kelley, L.A., Sternberg, M.J. (2010). 3DLigandSite: predicting ligand-binding sites using similar structures. *Nucleic Acids Res.* 38, 469–473.